

# Measuring anharmonicity in a large amplitude pendulum

Salvador Gil<sup>a)</sup>

*Escuela de Ciencia y Tecnología, Universidad Nacional de San Martín, Campus Miguelete, M. de Irigoyen 3100, San Martín (1650), Buenos Aires, Argentina*

Andrés E. Legarreta

*Departamento de Ingeniería Eléctrica, Universidad Tecnológica Nacional, Facultad Regional (1179), Buenos Aires, Argentina*

Daniel E. Di Gregorio

*Escuela de Ciencia y Tecnología, Universidad Nacional de San Martín, Campus Miguelete, M. de Irigoyen 3100, San Martín (1650), Buenos Aires, Argentina and Laboratorio Tandar, Departamento de Física, Comisión Nacional de Energía Atómica (1650), Buenos Aires, Argentina*

(Received 2 November 2007; accepted 23 March 2008)

We investigate the anharmonicity of a large amplitude pendulum and develop a novel technique to detect the high Fourier components as a function of the amplitude for large amplitudes close to  $180^\circ$ . The technique involves doing a Fourier analysis on each half-cycle of the amplitude versus time. The presence of the third and fifth harmonics is detected and the variations of the corresponding Fourier coefficients with amplitude are studied. The experimental setup is inexpensive and simple to implement. © 2008 American Association of Physics Teachers.  
[DOI: 10.1119/1.2908184]

## I. INTRODUCTION

The motion of a pendulum is harmonic only for very small angular deflections. At larger amplitudes nonlinear effects become more important.<sup>1-3</sup> The precision of modern laboratory equipment such as photogates and shaft encoders allows us to detect the effects of nonlinearity with simple and low cost equipment.<sup>4</sup> The effects of nonlinearity and the dependence of the period of the pendulum on amplitude have been discussed in several publications.<sup>5-8</sup> In contrast, experimental and theoretical studies on the spectral composition of the angular deflection of the pendulum as a function of time,  $\theta(t)$ , are more limited.<sup>9-11</sup> Previous studies have detected only the third harmonic, and agreement with the theoretical prediction was observed up to a maximum amplitude  $\theta_0$  less than about 2.2 rad.<sup>11</sup> In the rest of the text, angles will be expressed in radians unless otherwise indicated.

The purpose of this work is to measure the Fourier components of  $\theta(t)$  as a function of the maximum amplitude of the pendulum,  $\theta_0$ , and to compare these results with theory. To do this study we developed a novel technique for extracting the Fourier coefficients of a signal that has a period (fundamental frequency) which changes with time. The technique consists of doing a Fourier analysis on each half-cycle of the amplitude versus time. This technique is discussed in detail in the Appendix and is applied to the experimental deflection as a function of the time and the solution of the differential equation that describes the motion of the pendulum.

## II. THEORETICAL CONSIDERATIONS

In the absence of friction, the equation of motion of a physical pendulum is<sup>1-3</sup>

$$\frac{d^2\theta}{dt^2} + \omega_0^2 \sin(\theta) = 0, \quad (1)$$

where  $\omega_0^2 = mgd_{cm}/I$  is the natural frequency of the pendulum in the limit of very small amplitudes  $\theta_0$ . As usual,  $m$  is the

mass of the pendulum,  $I$  is the moment of inertia of the physical pendulum relative to the pivot,  $d_{cm}$  is the distance from this point to the center of gravity of the physical pendulum, and  $g$  is the acceleration of gravity. The angle  $\theta$  is the deflection of the pendulum with respect to the vertical that passes through the pivot.

Although there is a closed analytical solution of Eq. (1) in terms of the Jacobian elliptical functions,<sup>3</sup> it is simpler and more convenient to our purpose to solve Eq. (1) using a perturbative approach.<sup>2,7,10,12</sup> This technique consists of expanding  $\sin \theta$  in a Maclaurin series, and then solving Eq. (1), recursively. If the initial conditions are  $\theta(0) = \theta_0$  and  $\dot{\theta}(0) = 0$ , the solution of Eq. (1) is<sup>7,8,10-14</sup>

$$\begin{aligned} \theta(t) \approx & \theta_0 \cos \omega t + \frac{\theta_0^3}{192} (\cos \omega t - \cos 3\omega t) \\ & + \frac{\theta_0^5}{512} [(17/120)\cos \omega t - (1/6)\cos 3\omega t \\ & + (1/40)\cos 5\omega t] + \dots, \end{aligned} \quad (2)$$

with

$$\omega_0^2 \approx \omega^2 [1 + \theta_0^2/8 + 17\theta_0^4/1536 + \dots]. \quad (3)$$

Equation (2) can also be written as

$$\theta(t) = \sum_{n=0}^{\infty} A_{2n+1}(\theta_0) \cos[(2n+1)\omega t], \quad (4)$$

with

$$A_1(\theta_0) = \theta_0 + \theta_0^3/192 + (17/120)\theta_0^5/512 + \dots, \quad (5)$$

$$\begin{aligned} A_3(\theta_0) = & -[\theta_0^3/192 + (1/6)\theta_0^5/512 + \dots] \\ = & -(A_1^3/192)[1 + A_1^2/16 + \dots], \end{aligned} \quad (6)$$

$$A_5(\theta_0) = (1/40)\theta_0^5/512 + \dots = A_1^5/20480 + \dots, \quad \text{etc.} \quad (7)$$

The  $A_n$  may be identified as the Fourier coefficients of the spectral decomposition of  $\theta(t)$ . As expected, for very small amplitudes, the motion of the pendulum is harmonic with frequency  $\omega_0$ . As the amplitude increases, the nonlinear terms become important and produce a variation of the frequency (period) and the odd harmonic terms in  $\theta(t)$  become increasingly more important. To detect this effect experimentally, we could in principle use a pendulum with negligible friction, measure  $\theta(t)$ , and then Fourier analyze  $\theta(t)$ . In practice, it is difficult to build a sufficiently frictionless pendulum. Therefore, each half-cycle of the pendulum will have a different amplitude and a different fundamental frequency, which makes detecting the high harmonic frequencies difficult.

In the perturbative approach the expansion parameter is  $\theta$ . We would expect that the results deduced from this approach will be valid for  $\theta_0 < 1$  ( $\approx 57^\circ$ ) and when the effect of damping is negligible. In this study we will be able to explore larger amplitudes, for which the anharmonic effect is even larger, and to test the range of applicability of the perturbative solution.

As the amplitude increases, the characteristic velocity of the pendulum also increases. Thus, the effects of viscous and turbulent friction,<sup>4</sup> which depend on the velocity and the square of the velocity, respectively, also increase. Therefore, for large amplitudes ( $\theta_0 \approx \pi$ ) the effect of friction cannot be neglected, in general. In this case the equation of motion of the pendulum can be written as<sup>4</sup>

$$\frac{d^2\theta}{dt^2} = -\omega_0^2 \sin(\theta) - 2\gamma \frac{d\theta}{dt} - \beta \left| \frac{d\theta}{dt} \right|, \quad (8)$$

where  $\gamma$  and  $\beta$  are parameters associated with the strength of the viscous and turbulent components of the damping force, respectively. The turbulent contribution to the friction force is relevant whenever the Reynolds number of the motion of the pendulum in air is of the order of or larger than 4000,<sup>4</sup> which in our case was almost always the case, especially at large amplitudes. Equation (8) does not have an analytical solution, but can be solved numerically. However, there is an approximate expression that describes the amplitude of the pendulum as a function of time.<sup>4</sup> As expected, the turbulent component is more relevant when the amplitude is large, and consequently, the characteristic velocities are also large. As the amplitude decreases, the viscous component dominates, leading to an exponential decrease in the amplitude as a function of time. A simple program for solving this equation using MATLAB<sup>15</sup> was written; the numerical solution is denoted by  $\theta_T(t)$ . The parameters  $\omega_0$ ,  $\gamma$ , and  $\beta$  were obtained from the fit of the experimental data of  $\theta(t)$ . The parameters  $\omega_0$ ,  $\gamma$  and  $\beta$  are the only adjustable parameters. Of course,  $\omega_0$  could be calculated from the geometry of the pendulum as indicated in Eq. (1). Due to the complex geometry of our pendulum, we obtained  $\omega_0$  from the small angle oscillations of the pendulum. Our pendulum was optimized to study the large amplitude effects rather than to measure the value of  $g$  with great precision.<sup>4</sup> Once we obtained the parameters of  $\theta_T(t)$  that reproduced the experimental data, we did a Fourier analysis of each half cycle of this solution, using the procedure discussed in the Appendix. This procedure yields the amplitude  $\theta_0$  and the Fourier coefficients  $A_n$  associated with each half cycle.

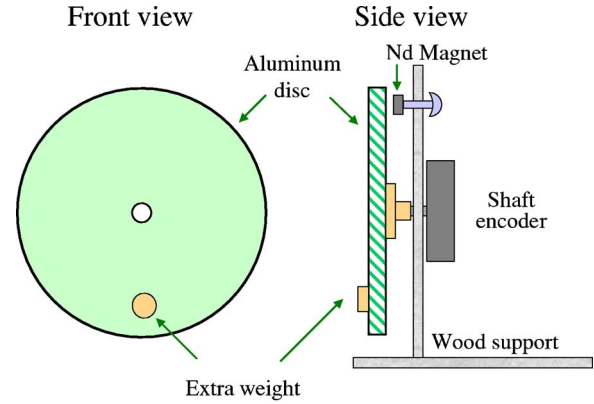


Fig. 1. The experimental setup consists of an aluminum disk suspended at its center. It is fixed to the axis of an optical shaft encoder. An extra weight can be placed on the face of the disk close to its edge to break its mass symmetry. A neodymium magnet is used to vary the “viscous” friction coefficient.

### III. THE EXPERIMENT

The pendulum consists of an aluminum disk, 29.5 cm in diameter and 3 mm thick, suspended at its center. The disk with its fixation hub, weigh 967 g. It is fixed to the axis of a shaft encoder as shown in Fig. 1. An extra weight of 50 or 100 g can be fastened with a brass bolt placed on the face of the disk close to its edge to break the mass symmetry of the system. The disk has several holes, evenly spaced in a radial direction, allowing the distance of the weight to its center to be changed. The magnitude of the weight also can be changed. By manipulating the position and magnitude of the weight we could choose the period of the pendulum at very small amplitudes. A neodymium magnet (diameter 12.7 mm and 6.35 mm thick; grade N40) can be placed at 10 cm from the axis of rotation. Its distance to the disk can be regulated with a bolt. In this manner the friction coefficient (proportional to the velocity) can be changed. An optical shaft encoder<sup>16</sup> connected to a computer, with an angular resolution of 0.3 degrees, was used to monitor the angular position of the pendulum. The estimated error in the determination of the angles was at most 0.5 degrees. Because error bars associated with these uncertainties would be smaller than the size of the symbols used to represent the data, they are not shown in Figs. 2–4.

Due to the very low friction of the shaft encoder and the large mass of the pendulum, the motion persisted for more than 250 oscillations. The angles measured at a rate of 20 Hz, so about 60 data points were characterized every period. The mechanical design of the pendulum is similar to the arrangement used in Ref. 17.

### IV. RESULTS AND DISCUSSION

In Fig. 2 we display  $\theta_e(t)$  (diamond symbols), the experimentally measured angles as a function of time for  $\theta_0 \approx \pi$ . The continuous line in Fig. 2 is a single frequency cosine function which has the same period and amplitude as the pendulum. The deviation of the experimental results from the cosine reveals the presence of higher harmonic components.

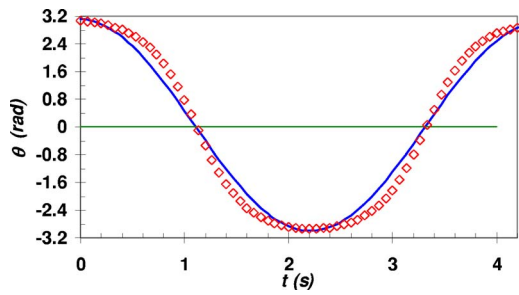


Fig. 2. Angular deflection as a function of time for the frictionless pendulum, when its amplitude is close to  $\pi$ . The diamond symbols are the experimental data. The continuous line is a single frequency cosine function that has the same period and amplitude as that of the pendulum. The deviation of the experimental results from the cosine function reveals the presence of higher harmonics.

In Fig. 3 we show  $\theta_e(t)$  for a longer time, together with the numerical solution of Eq. (2) with the two friction terms. The effects of the nonlinearity, revealed in the lack of isochronism of the pendulum, are clearly seen. The period of the first and fifth cycles is 4.2 and 3.2 s, respectively.

We used the algorithms described in the Appendix to Fourier analyze the measured deflection,  $\theta_e(t)$ , for each half-cycle. We thus explored the variation of the Fourier coefficients,  $A_n$ , for the fundamental frequency and its harmonics, as a function of the amplitude  $\theta_0$ . Figure 4 shows the variation of  $A_1$  (associated with the fundamental frequency) and  $A_3$  with  $\theta_0$ . Similarly, Fig. 5 shows the variation of  $A_5$ , and  $A_7$  as a function of the amplitude. In Figs. 4 and 5 the symbols represent the Fourier coefficients extracted from  $\theta_e(t)$ , and the continuous lines are the corresponding predictions from the model. In Figs. 4 and 5 we show the behavior of  $A_1$ ,  $A_3$ ,  $A_5$ , and  $A_7$  versus  $\theta_0$  obtained by a Fourier analysis on  $\theta_T(t)$ . The latter was obtained by solving Eq. (8) numerically with parameters that reproduce the experimental results,  $\theta_e(t)$ , as illustrated in Fig. 2. We see that the model provides an adequate description of the experimental data for all the amplitudes studied. In Figs. 4 and 5 we also show the theoretical expectation (dotted lines) obtained using the perturbation approach, Eqs. (4)–(7), which reproduce the data only for  $\theta_0 < 2.2$ . A similar lack of agreement between the perturbative approach and the experimental results is visible in the pioneering work of Zilio.<sup>11</sup> Because the expansion parameter is  $\theta$  in the perturbative approach,<sup>2,7,8,12,14</sup> our expectation was that Eqs. (5)–(7) would break down for  $\theta_0$  of the order of 1.

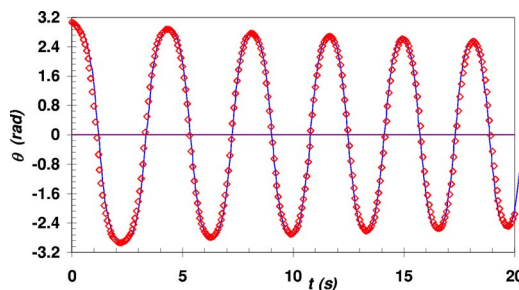


Fig. 3. Angular deflection as a function of time for the free pendulum. The diamond symbols are the experimental data and the continuous line is the result of the model including friction, obtained by solving Eq. (8) numerically, with parameters that reproduce the experimental results.

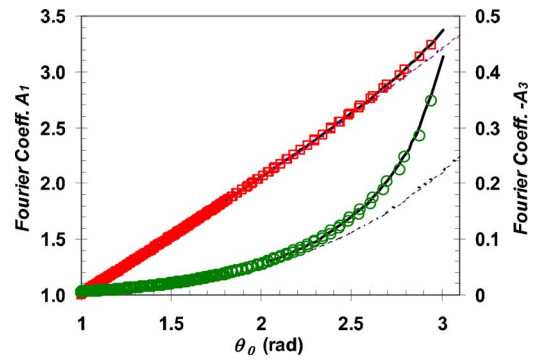


Fig. 4. Fourier coefficients versus the amplitude. The first harmonic,  $A_1$ , is referenced to the left vertical axis, and those associated to the third harmonics,  $A_3$ , are referenced to the right vertical axis. The symbols (open squares and circles) represent the Fourier coefficients obtained from the experimental data of  $\theta_e$  versus  $t$ . The dotted lines are the predictions of the perturbation approach in Eq. (5). The heavy continuous lines represent the results of a half-cycle Fourier analysis of the theoretical solution,  $\theta_T(t)$ , obtained by solving Eq. (8).

As can be observed in Figs. 4 and 5, the perturbative solution reproduced the experimental data quite well even for amplitudes close to 2.2. Up to this angle, the differences between the solid lines, the dotted curves, and the experimental data are less than the experimental uncertainties. The Fourier coefficients obtained with the perturbative approach were consistent with the coefficients obtained using the half-cycle analysis of the numerical solution of Eq. (1) when the damping was suppressed. The presence of damping leads to the temporal variation of the amplitude, period, and the dependence of the Fourier coefficients as a function of the amplitude. Figure 5 illustrates this variation, and we see that the difference between the theoretical approaches becomes important for only  $\theta_0 > 2.2$ . For angles close to  $\pi$ , the Fourier analysis of the numerical solution of Eq. (8) provides a much better description of the experimental data than the perturbative approach, carried out up to the fifth order.

In summary, we have constructed a pendulum to investigate the behavior of the Fourier coefficients as a function of the amplitude. We were able to detect the third and fifth harmonics and marginally the seventh harmonic for ampli-

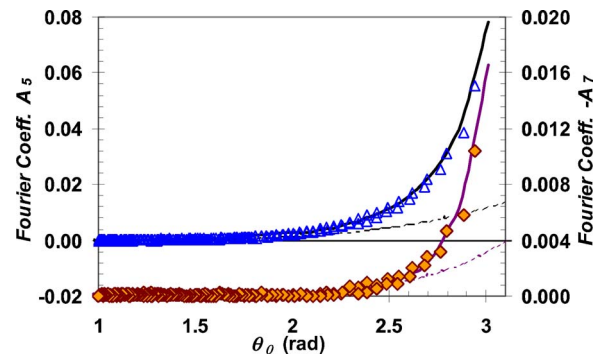


Fig. 5. Fourier coefficients versus the amplitude. The fifth harmonic,  $A_5$ , is referenced to the left vertical axis, and the seventh harmonic,  $A_7$ , is referenced to the right vertical axis. The symbols (open triangles and rhomboids) are the Fourier coefficients obtained from the measured angular deflection. The dotted lines are the predictions of the perturbation approach, given in Eqs. (6) and (7), respectively. The heavy continuous lines represent the results of a Fourier analysis on  $t \theta_T(t)$ , obtained by solving Eq. (8).

tudes close to  $\pi$ . The experimental result is consistent with the results predicted by the model, for angular amplitudes up to 3. The setup is inexpensive and is simple to construct. The experiment can be done in intermediate laboratory courses to illustrate important consequences of a nonlinear system.

## ACKNOWLEDGMENTS

We gratefully acknowledge the valuable comments and suggestions made by Dr. E. Batista. We are also grateful to Dr. A. Schwint for careful reading of the manuscript and to H. Dipaolo for his assistance in the construction of our pendulum. We are also grateful to the two anonymous referees for their constructive review and very valuable suggestions that helped to improve the quality of this paper.

## APPENDIX: HALF-CYCLE FOURIER ANALYSIS

We summarize the algorithm used for doing the half-cycle Fourier analysis of the measured angular deflection  $\theta_e(t)$ , and the numerical solution  $\theta_T(t)$  of the differential equation in Eq. (8). The basic characteristics of  $\theta(t)$  are that its period and amplitude decrease monotonically with time, as shown in Fig. 3. Because the raw data collected with the data acquisition system are not evenly spaced in time, a spline interpolation was done. This interpolation generates a new set of angles evenly spaced in time at a rate of about 200 Hz. Next, the zero crossing times of the signal are searched. With this information a set of half-cycles or semicycles are defined, comprising two consecutive zeros and all the values interpolated from the measured angles, within these time intervals,  $\theta^{(k)}(t)$ . The absolute value of  $\theta^{(k)}(t)$  is then found for each semicycle.

The maximum of each semicycle is the amplitude  $\theta_0^{(k)}$ . Next, a complete pseudocycle is constructed for each semicycle, whose period  $T^{(k)}$  is twice the difference between two adjacent zeros that define each semicycle. The superindex ( $k$ ) characterizes each pseudocycle. The pseudocycle comprises the corresponding semicycle and its reflection,

$$\theta^{(k)}(t) = \begin{cases} \theta^{(k)}(t) & \text{if } 0 \leq t \leq T^{(k)}/2 \\ -\theta^{(k)}(T^{(k)} - t) & \text{if } T^{(k)}/2 < t < T^{(k)}. \end{cases} \quad (\text{A1})$$

For each semicycle ( $k$ ) we obtain a complete pseudocycle, characterized by a vector  $\theta_j^{(k)}$  of dimension  $N^{(k)}$ , representing the angular position of the pendulum at evenly spaced time intervals. A Fourier analysis is done on each pseudocycle, and the Fourier coefficients  $A_n$  are calculated as<sup>18</sup>

$$\begin{aligned} A_n^{(k)} &= \frac{2}{T^{(k)}} \int_0^{T^{(k)}} \theta(t) \exp\left(-i \frac{2\pi n}{T^{(k)}} t\right) dt \\ &\approx \frac{2}{N^{(k)}} \sum_{l=0}^{N^{(k)}-1} \theta_l^{(k)} \exp(-i 2\pi n l / N^{(k)}). \end{aligned} \quad (\text{A2})$$

As a consequence of the symmetry property in Eq. (A1), only the odd Fourier coefficients will be nonzero. Using this procedure we are able to extract, for each half-cycle ( $k$ ), an amplitude,  $\theta_0^{(k)}$ , a period,  $T^{(k)}$ , and the Fourier coefficients  $A_n^{(k)}$ .

To test the reliability of our method, we used our MATLAB program on an artificial signal with a known Fourier coefficients. Let us define a signal function,

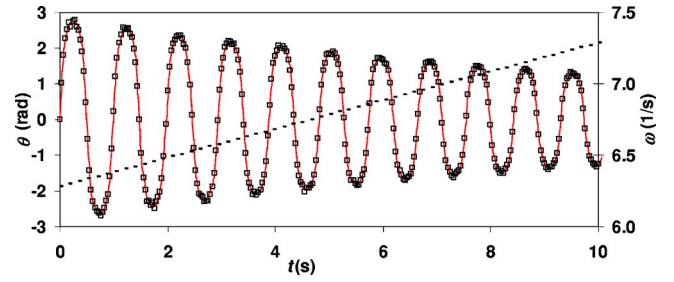


Fig. 6. Artificial angular deflection. The thin continuous line represents the artificial angular signal, Eq. (A3). The square symbols are the artificial data, including randomness, obtained using Eq. (A7). The dashed line represents the variation in the angular frequency  $\omega(t)$  with time, referred to the right vertical axis, Eq. (A4).

$$\begin{aligned} f_T(t) &= A_0 \exp(-\gamma t) [\sin(\phi(t)) + B_3 \sin(3\phi(t)) \\ &\quad + B_5 \sin(5\phi(t)) + B_7 \sin(7\phi(t))], \end{aligned} \quad (\text{A3})$$

with

$$\phi(t) = \int_0^t \omega(u) du \quad \text{and} \quad \omega(t) = \omega_0(1 + a_0 t). \quad (\text{A4})$$

Here,  $\omega_0$  and  $a_0$  are constants that generate a signal with variable frequency or period. The constants  $A_0$ ,  $\gamma$ ,  $B_3$ ,  $B_5$ , and  $B_7$  are chosen to simulate actual data. The function given by Eq. (A3) represents a signal that has variable frequency and variable Fourier components

$$A_1^{(t)} = \text{fundamental frequency amplitude} = A_0 \exp(-\gamma t), \quad (\text{A5})$$

$$A_3^{(t)} = \text{third harmonic amplitude} = A_0 \exp(-\gamma t) B_3, \quad (\text{A6})$$

and so on.

The signal described by Eq. (A1) is an artificial signal created to mimic the characteristics of a real signal. Its Fourier coefficients have a known dependence on time and amplitude, Eqs. (A5) and (A6), but are not expected to match

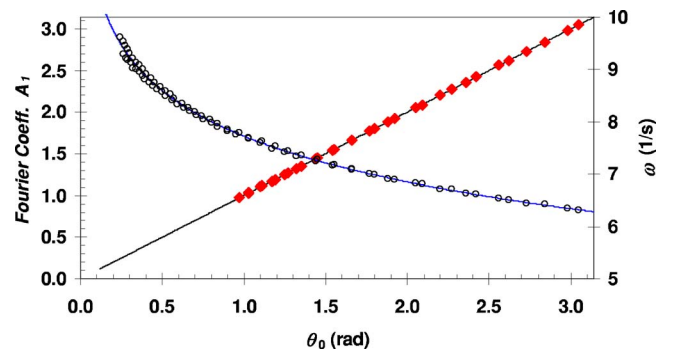


Fig. 7. Frequency and first Fourier coefficient as a function of the amplitude for the artificial signal. The continuous curves are theoretical inputs, Eqs. (A4) and (A5). The symbols are the results obtained using our half-cycle Fourier analysis of the artificial signal given by Eq. (A8) as input and with  $\sigma=2\%$ . The artificial signal mimics the basic characteristics of a real signal, but is not expected to match the pendulum data. The circles represent the Fourier coefficients  $A_1$ , referred to the left vertical axis and the rhomboidal symbols are the frequencies, extracted from the artificial signal, referred to the right vertical axis.

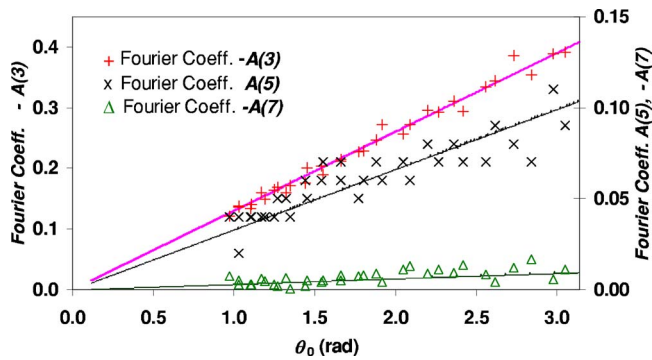


Fig. 8. Fourier coefficients as a function of amplitude for the artificial signal.  $A_i$  is the Fourier coefficient associated with the  $i$ th harmonic. The continuous curves are theoretical inputs obtained using Eq. (A4). The symbols are the results obtained using our half-cycle Fourier analysis of the artificial signal given by Eq. (A8) with  $\sigma=2\%$ .

exactly the actual pendulum data. This artificial signal can be used as a test of the performance of our half-cycle Fourier analysis.

To introduce some randomness into the artificial signal we use a simplified version of the Monte Carlo technique. If  $\sigma$  represents the characteristic magnitude of the relative dispersion of the data, a new signal is defined as

$$f_{\text{artif}}(t) = f_T(t) + \Delta f_{\text{random}} = f_T(t) + (f_T \sigma) r = f_T(t) [1 + r\sigma], \quad (\text{A7})$$

where  $r$  is a random number taken from a Gaussian distribution with the mean equal to 0 and standard deviation equal to 1. The artificial signal resembles the one we would like to study, but with known behavior and parameters, because the values  $\gamma$ ,  $\omega_0$ ,  $a_0$ ,  $B_i$ , and  $\sigma$  are known. To test our Fourier analysis method we introduced the function in Eq. (A7) into our program and compared the Fourier coefficients thus obtained with the input parameters, defined by Eqs. (A4)–(A6). In Fig. 6 we present an example of the artificial signal using  $\sigma=2\%$ .

The results of the Fourier analysis of the synthetic signal are summarized in Figs. 7 and 8. We see that for a signal with a relative dispersion of  $\sigma=2\%$ , considerably larger than the dispersion we expect in our actual data, we are able to

obtain the first three odd harmonics. Hence, we expect that the half-cycle Fourier analysis proposed in this work is adequate for detecting the third, fifth, and seventh Fourier coefficients of magnitude comparable to the one observed in our actual data, Figs. 4 and 5.

<sup>a)</sup>Electronic mail: [sgil@df.uba.ar](mailto:sgil@df.uba.ar)

<sup>1</sup>Stefen T. Thornton and Jerry B. Marion, *Classical Dynamics of Particles and Systems*, 5th ed. (Brooks/Cole, New York, 2004), Vol. 1, p. 153.

<sup>2</sup>Herbert Goldstein, Charles P. Poole, and John F. Safo, *Classical Mechanics*, 3rd ed. (Addison-Wesley, Boston, 2001), Vol. 1, p. 483.

<sup>3</sup>Ted C. Bradbury, *Theoretical Mechanics* (John Wiley & Sons, New York, 1968), Vol. 1, p. 222.

<sup>4</sup>R. A. Nelson and M. G. Olsson, “The pendulum—Rich physics from a simple system,” *Am. J. Phys.* **54**(2), 112–121 (1986).

<sup>5</sup>F. M. S. Lima and P. Arun, “An accurate formula for the period of a simple pendulum oscillating beyond the small angle regime,” *Am. J. Phys.* **74**(10), 892–895 (2006).

<sup>6</sup>R. B. Kidd and S. L. Fogg, “A simple formula for large-angle pendulum period,” *Phys. Teach.* **40**, 81–83 (2002).

<sup>7</sup>S. Gil and D. E. DiGregorio, “Perturbation of a classical oscillator: A variation on a theme of Huygens,” *Am. J. Phys.* **74**(1), 60–67 (2006).

<sup>8</sup>L. P. Fulcher and B. F. Davis, “Theoretical and experimental study of the motion of the simple pendulum,” *Am. J. Phys.* **44**(1), 51–55 (1976).

<sup>9</sup>R. Simon and R. P. Riesz, “Large amplitude simple pendulum: A Fourier analysis,” *Am. J. Phys.* **47**, 898–899 (1979).

<sup>10</sup>Donald E. Hall, “Comments on Fourier analysis of the simple pendulum,” *Am. J. Phys.* **49**(8), 792–792 (1981).

<sup>11</sup>S. C. Zilio, “Measurement and analysis of large-angle pendulum motion,” *Am. J. Phys.* **50**(5), 450–452 (1982).

<sup>12</sup>L. A. Pipes and L. R. Harvill, *Applied Mathematics for Engineers and Physicists*, 3rd ed. (McGraw-Hill, New York, 1970), Vol. 1, p. 995.

<sup>13</sup>There is an apparent discrepancy between the results of the perturbation method, Eqs. (2), (3), (5), and (7), presented here and in Ref. 8 and the results of Ref. 11. If the typos in Ref. 11 are taken into account, the two results are the same. We are grateful to one of the referees for pointing out this apparent disagreement.

<sup>14</sup>A. Beléndez, A. Hernández, T. Beléndez, C. Neipp, and A. Márquez, “Application of the homotopy perturbation method to the nonlinear pendulum,” *Eur. J. Phys.* **28**(1), 93–104 (2007).

<sup>15</sup>Further details of our experiment and a copy of the MATLAB program for the Fourier analysis of the experimental results and for solving numerically Eq. (8) can be obtained from ([www.fisicarecreativa.com](http://www.fisicarecreativa.com)).

<sup>16</sup>US Digital, 1400 NE 136th Ave., Vancouver, WA 98684, ([www.usdigital.com](http://www.usdigital.com)).

<sup>17</sup>Y. Kraftmakher, “Computerized physical pendulum for classroom demonstration,” *Phys. Teach.* **43**, 244–246 (2005).

<sup>18</sup>Hwe P. Hsu, *Applied Fourier Analysis* (Int. Thompson, New York, 1984).